ACS OMEGA

Article

Cite This: ACS Omega 2019, 4, 15560−15566

http://pubs.acs.org/journal/acsodf

Integrin α6-Targeted Positron Emission Tomography Imaging of Colorectal Cancer

Yi-Tai Xiao,[†,∥] Chao Zhou,[‡,∥] Jia-Cong Ye,[§,∥] Xiao-Chun Yang,[‡] Zhi-Jian Li,[‡] Xiao-Bin Zheng,[‡] Yan Mei,[§] Xin-Ling Li,[‡] Wei-Guang Zhang,[‡] Wei Fan,[‡] Mu-Sheng Zeng,[§] Jian-Jun Li,*[,†] and Guo-Kai Feng*[,§]

[†]Department of Endoscopy, State Key Laboratory of Oncology in South China, Collaborative Innovation Center for Cancer Medicine, [‡]Department of Nuclear Medicine, State Key Laboratory of Oncology in South China, Collaborative Innovation Center for Cancer Medicine, and [§]Department of Experiment, State Key Laboratory of Oncology in South China, Collaborative Innovation Center for Cancer Medicine, Sun Yat-sen University Cancer Center, Guangzhou 510060, China

Supporting Information

ABSTRACT: Colorectal cancer (CRC) is the third most common cancer and the fourth leading cause of cancer deaths worldwide. Integrin α6 is overexpressed in all stages of CRC which makes it a potential diagnostic biomarker for CRC. Previously, we identified an integrin α6-targeted peptide CRWYDENAC (dubbed RWY) using phage display technology and employed it for nasopharyngeal carcinoma specific nanotherapeutics. In this study, we developed a radiotracer, ^{18}F-RWY, based on this integrin α6-targeted RWY peptide for positron emission tomography (PET) imaging of CRC. Integrin α6 was overexpressed on several CRC cells including HT29 cells where the biotin-labeled RWY peptide colocalized with integrin α6. ^{18}F-RWY PET imaging was performed on subcutaneous, chemically induced, and genetically engineered CRC mice. ^{18}F-RWY generated high PET signals in subcutaneous HT29 tumors, and the tumor uptake of ^{18}F-RWY was reduced by a blocking study using nonradio-labeled RWY. Moreover, ^{18}F-RWY PET imaging enabled detection of CRC in chemically induced and genetically engineered CRC mice. The overexpression of integrin α6 in tumor tissues isolated from chemically induced and genetically engineered CRC mice was confirmed. These results demonstrate the potential clinical application of ^{18}F-RWY for PET imaging of CRC.

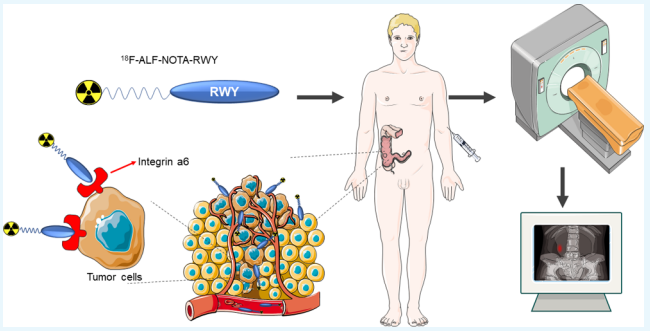

INTRODUCTION

Colorectal cancer (CRC), which accounted for 1.7 million new cases and more than 800 000 deaths in 2018, is the third most common cancer worldwide and the fourth leading cause of cancer deaths, with its incidence increasing each year.[1,2] Surgical resection is an effective treatment for patients with localized stage CRC, with a 5-year survival rate of up to 90% being observed.[2] Early diagnosis of CRC is critical for the choice of follow-up treatment and prognosis of patients. Currently, the gold standard for the diagnosis of CRC relies on the pathological report of the biopsy samples taken during endoscopy. Complete colonoscopy or computed tomography (CT) colonoscopy is necessary for the staging of CRC. As a noninvasive method of tumor detection, positron emission tomography/CT (PET/CT) is crucial for the performance of presurgical staging and identification of metastatic or recurrent lesions.[3] PET/CT has been shown to alter the therapy of nearly one-third of patients with advanced primary rectal cancer.[4]

^{18}F-Fluorodeoxyglucose (^{18}F-FDG) is the most widely clinically used PET radiotracer for the detection of cancers. The growth and proliferation of malignant cells are active and accelerated, and glucose utilization and glycolysis are significantly increased. Therefore, the concentration of deoxyglucose in tumor cells is significantly higher than that in normal cells.[5] As an important organ for nutrient absorption, the colon is adjacent to the small intestine, where glucose uptake is active, and physiological glucose uptake in the gastrointestinal tracts may lead to misinterpretation of PET/CT results of ^{18}F-FDG.[4] In addition, some organs with high glucose metabolism, such as the brain and the heart, often show a high standardized uptake value (SUV) in ^{18}F-FDG based PET images, which makes it difficult to distinguish the metastases of these organs.[6]

Integrin α6 is a subtype of the integrin family, which is expressed on the surface of cells and acts as a regulator of a variety of cellular functions that are critical to the occurrence, development, and metastasis of solid tumors.[7] Several studies

Received: June 26, 2019
Accepted: August 28, 2019
Published: September 11, 2019

DOI: 10.1021/acsomega.9b01920
ACS Omega 2019, 4, 15560−15566

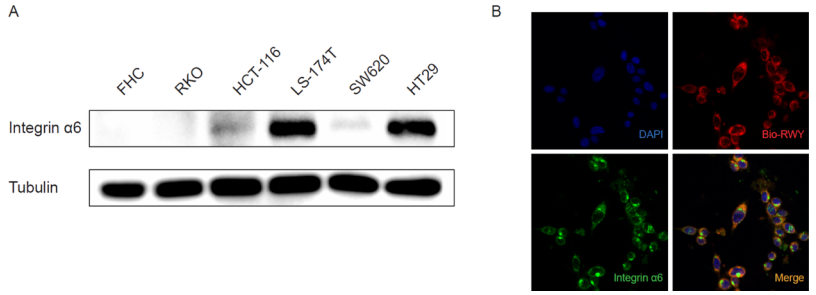

Figure 1. Integrin $\alpha 6$-target peptide binds to CRC cells. (A) Expression of integrin $\alpha 6$ in the normal intestinal epithelial cell line (FHC) and CRC cell lines (HT29, LS-174T, RKO, HCT116, and SW620) were examined by western blotting. (B) Cellular fluorescent imaging of HT29 cells incubated with biotin-labeled RWY peptide at 37 °C for 2 h. Blue, DAPI; red, bio-RWY; green, integrin $\alpha 6$.

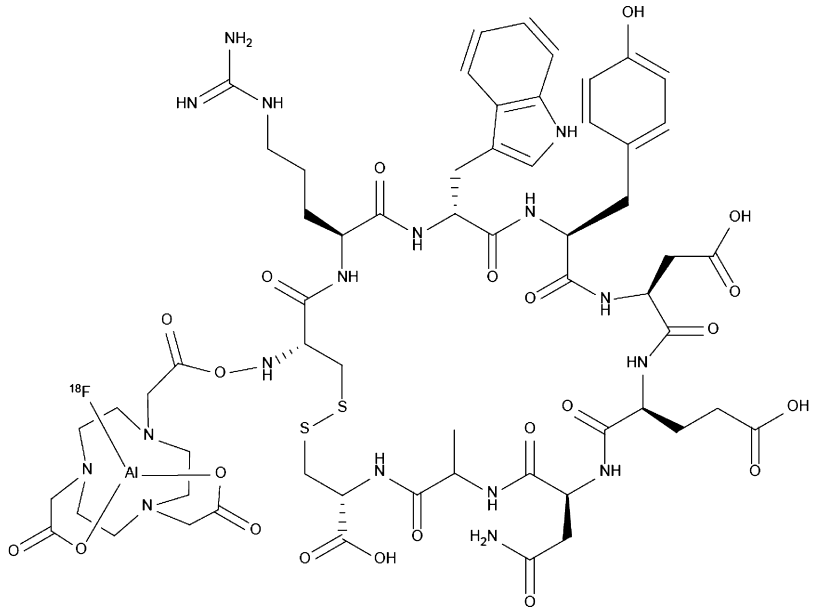

Figure 2. Chemical structure of ^{18}F-AlF-NOTA-RWY (^{18}F-RWY). The 1,4,7-triazacyclononanetriacetic acid (NOTA)-conjugated RWY peptide was radiolabeled with radionuclide fluorine-18 (^{18}F).

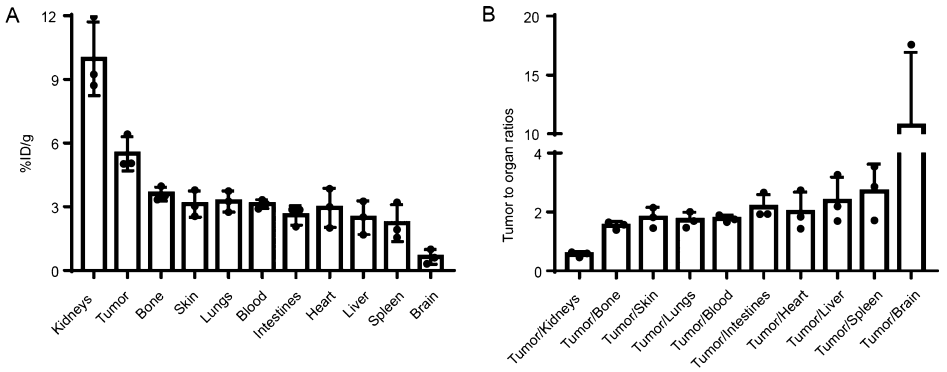

Figure 3. In vivo biodistribution of ^{18}F-RWY in subcutaneous HT29 tumor-bearing mice. (A) A γ counter was used to quantify the ^{18}F-RWY uptakes in tumor tissues and normal tissues and organs (n = 3). (B) Tumor-to-organ ratios of ^{18}F-RWY at 60 min postinjection (n = 3).

have reported the prognostic significance of integrin $\alpha 6$ in several tumors including hepatocellular carcinoma,[8] breast cancer,[9] and bladder cancer.[10] Previously, we identified a tumor-targeted peptide CRWYDENAC (dubbed RWY) using phage display technology and further confirmed its target as integrin $\alpha 6$.[11] Many studies have suggested that integrin $\alpha 6$ is overexpressed in CRC, and its overexpression is associated with the development of more aggressive and metastatic phenotypes in CRC cells.[12,13] The notably high expression level of integrin $\alpha 6$ in CRC makes it a potential target for molecular imaging of CRC. In this study, we develop an integrin $\alpha 6$-targeted RWY-based PET radiotracer ^{18}F-ALF-NOTA-RWY (dubbed ^{18}F-RWY for short) for PET imaging of CRC in subcutaneous, genetically engineered and chemically induced CRC mice.

DOI: 10.1021/acsomega.9b01920
ACS Omega 2019, 4, 15560−15566

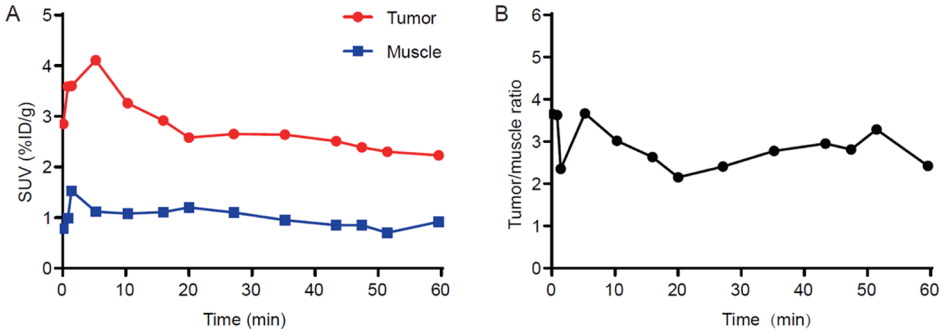

Figure 4. Dynamic PET imaging in subcutaneous HT29 tumor-bearing mice. (A) Dynamic PET imaging was performed for a period of 60 min (n = 3). Representative time activity of ^{18}F-RWY uptake in tumor and muscle tissue. (B) The representative tumor-to-muscle ratio was calculated (n = 3).

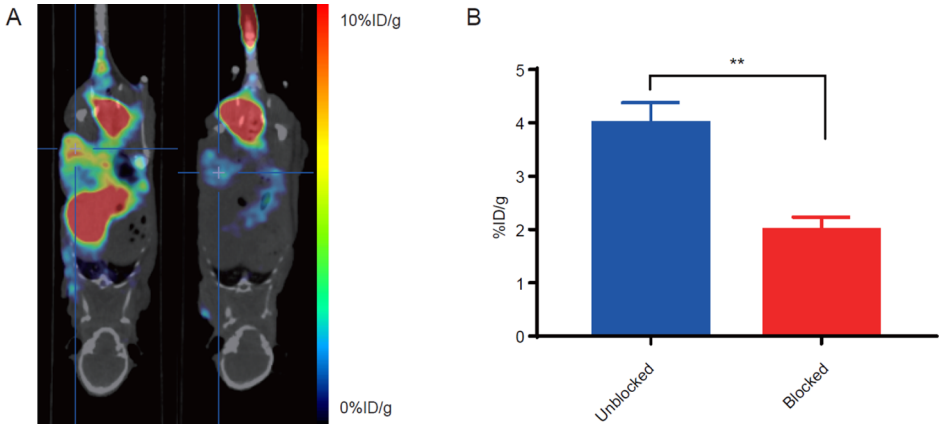

Figure 5. PET/CT imaging of the blocking study in subcutaneous HT29 tumor-bearing mice. (A) Representative PET/CT images of HT29 tumor-bearing mice after injection of ^{18}F-RWY only (left) or accompanied with a blocking dose of 1 mg of nonradiolabeled RWY peptide (right). (B) Quantification of radiotracer uptake in the tumor. The statistical analysis was performed using Student's t-test, n = 3, $^{**}p < 0.01$.

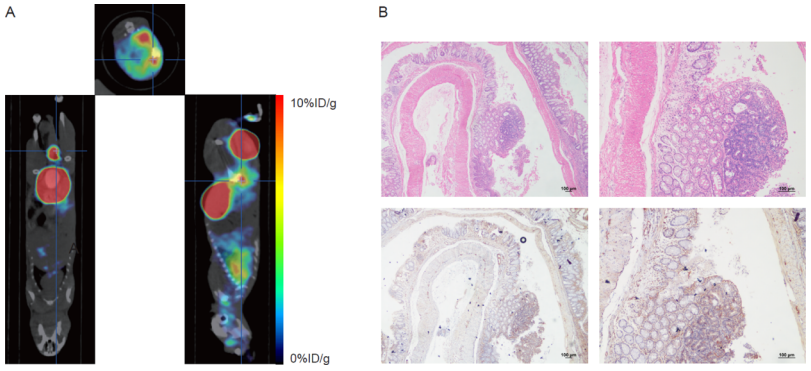

Figure 6. PET/CT imaging with ^{18}F-RWY in chemically induced CRC mice. (A) Representative PET/CT imaging with ^{18}F-RWY in a chemically induced CRC mouse. (B) H&E and immunohistochemistry staining of tumor isolated from a chemically induced CRC mouse. Integrin $\alpha 6$ expression was analyzed using immunohistochemistry. Scale bar, 100 μm.

RESULTS

Binding of RWY to CRC Cells. The expression levels of integrin $\alpha 6$ were examined on several CRC cells including RKO, HCT116, LS-174T, SW620 and HT29, and normal colorectal epithelial FHC cells. High expression of integrin $\alpha 6$ was observed in LS-174T and HT29 cells; medium expression in HCT116 and SW620 cells; and low expression in FHC and RKO cells (Figure 1A). The integrin $\alpha 6$-overexpressing CRC cell HT29 was used in our following studies. Confocal imaging showed that biotin-labeled RWY peptide colocalized with integrin $\alpha 6$ in HT29 cells (Figure 1B).

Development of an Integrin $\alpha 6$-Targeted PET Radiotracer. We synthesized a 1,4,7-triazacyclononanetriacetic acid (NOTA)-conjugated RWY peptide that was radiolabeled with radionuclide fluorine-18 (^{18}F) to form a PET radiotracer ^{18}F-ALF-NOTA-RWY (dubbed ^{18}F-RWY for short) (Figure 2), according to a previous report.[14] The stability of ^{18}F-RWY was determined by high-performance liquid chromatography (HPLC). A unique radioactive peak was observed by HPLC (Figure S1), indicating that ^{18}F-RWY was stable.

Biodistribution in a Subcutaneous CRC Mouse Model. Mice-bearing HT29 subcutaneous xenograft tumors

DOI: 10.1021/acsomega.9b01920
ACS Omega 2019, 4, 15560−15566

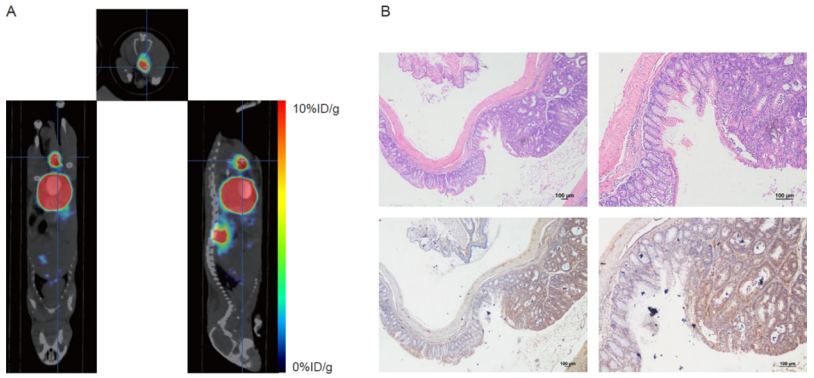

Figure 7. PET/CT imaging with ^{18}F-RWY in genetically engineered CRC mice. (A) Representative PET/CT imaging with ^{18}F-RWY in an $Apc^{min/+}$ genetically engineered CRC mouse. (B) H&E and immunohistochemistry staining of a tumor resected from an $Apc^{min/+}$ genetically engineered CRC mouse. Integrin $\alpha 6$ expression was analyzed using immunohistochemistry. Scale bar, 100 μm.

were intravenously injected with 3.7 MBq (100 μCi) of ^{18}F-RWY. Mice were sacrificed 60 min after intravenous injection. Tumor tissues and normal organs were harvested, weighed, and measured by a γ counter. Quantification indicated the highest radioactive accumulation of ^{18}F-RWY in the kidneys, suggesting it was predominantly cleared by the urinary system (Figure 3A). Tissue uptake in tumor tissues was higher than in other normal tissues and organs (including the bone, skin, lungs, blood, intestines, heart, liver, spleen, and brain) except for the kidneys (Figure 3B).

To analyze the dynamic distribution of ^{18}F-RWY in vivo, a dynamic PET/CT imaging was performed. The time activity curves for tumor and muscle were calculated. As shown in (Figure 4A), the accumulation of ^{18}F-RWY in the tumor reached peak in approximately 5 min and remained stable during 60 min postinjection. Similar trends were observed in muscle. Comparatively, the radiotracer uptake in the tumor was approximately three folds higher than that observed in muscle during 60 min postinjection (Figure 4B).

To further confirm the binding specificity of ^{18}F-RWY, an in vivo blocking assay was performed by tail vein injection of 1 mg of nonradiolabeled RWY peptide before injection of ^{18}F-RWY (Figure 5A). The PET signal in the tumor was dramatically reduced from 3.99 ± 0.22 to 1.99 ± 0.14 % ID/g (Figure 5B), suggesting that the tumor accumulation of ^{18}F-RWY was mediated by the RWY peptide.

PET/CT Imaging on Chemically Induced and Genetically Engineered CRC mice. In chemically induced CRC mice, ^{18}F-RWY showed high tumor uptake and low background uptake. Tumor uptake of ^{18}F-RWY was quantified as 5.87 ± 0.99 % ID/g (Figure 6A). In the 3D model image, the ^{18}F-RWY displayed excellent tumor enrichment (Figure S2). To further confirm the presence of the tumor, mice were sacrificed 24 h after PET/CT imaging until the radioactivity decayed to negligible amounts. The colon and rectum were collected for observations, including H&E staining as well as immunohistochemistry. Gross and microscopic observations showed that the tumor was successfully induced in the colon, which was also confirmed by H&E staining results. High integrin $\alpha 6$ expression in the tumor tissues was observed in the image of immunohistochemistry compared with that in the intestine adjacent to the tumor (Figure 6B).

In an $Apc^{min/+}$ genetically engineered CRC mouse, representative PET/CT and maximum intensity projection imaging displayed an excellent targeting effect of the ^{18}F-RWY. The maximum value of calculated tumor uptake was 5.74 ± 0.71 % ID/g (Figure 7A). In the 3D model image, the ^{18}F-RWY also showed excellent tumor targeting (Figure S3). Compared with ^{18}F-RWY, ^{18}F-FDG did not show ideal tumor enrichment. Instead, it was mainly enriched in some nonspecific sites, such as the heart, the brain, and the subcutaneous adipose tissue (Figure S4). H&E staining confirmed the presence of the tumor in the colon. Immunohistochemistry showed that tumor tissues showed relatively high expression of integrin $\alpha 6$ compared to the intestine tissues adjacent to the tumor (Figure 7B).

DISCUSSION

Previously, we identified a tumor-targeted peptide RWY using phage display technology and further confirmed its target as integrin $\alpha 6$.[11] Herein, we developed an integrin $\alpha 6$-targeted PET radiotracer, ^{18}F-RWY, and focused its application on CRC. The integrin $\alpha 6$-overexpressing CRC cells HT29 were used to establish subcutaneous CRC tumors. We confirmed that integrin $\alpha 6$ is the primary cellular target of the RWY peptide, and the RWY peptide binds to integrin $\alpha 6$ CRC cells in vitro. In the blocking assay, we further confirmed the specificity of ^{18}F-RWY binding to the subcutaneous tumor of CRC, thereby suggesting that ^{18}F-RWY can effectively and specifically accumulate in CRC tumors. We further validated the feasibility of ^{18}F-RWY for the detection of CRC in chemically induced and genetically engineered CRC mice as well. We finally confirmed the overexpression of integrin $\alpha 6$ in tumor tissues isolated from chemically induced and genetically engineered CRC mice.

Diagnosis and monitoring of CRC rely heavily on colonoscopy. Nevertheless, as an invasive technique, colonoscopy requires a long period of bowel preparation and anesthesia to reduce pain, which is intolerable for some patients.[15] Colonoscopy, on the other hand, is highly dependent on the experience of the operator, and detection of neoplasms in the occult site is often difficult because of blind spots.[16] Approximately 26% of neoplastic polyps was missed during single colonoscopy, according to a meta-analysis.[17] For verdant operators, unskilled manipulation is likely to lead to bleeding, perforation, and other severe complications. Therefore, more noninvasive approaches are still urgently needed to be explored for better diagnosis of CRC.

With the introduction and rapid development of precision medicine, it is necessary to explore tumor biomarkers that can

DOI: 10.1021/acsomega.9b01920
ACS Omega 2019, 4, 15560−15566

reflect changes on the tumor cell and subcell level before changes in the anatomic structure.[18,19] Because of the noninvasiveness, high sensitivity, and lack of blind spots, the PET imaging modality is widely accepted in oncological imaging. PET imaging based on tumor-targeting molecules has been rapidly developed and has achieved good results in many cancers.[19] ^{18}F-FDG, a PET radiotracer based on glucose metabolism, is the most widely used for oncological imaging. However, because of the abnormal absorbability of inflammatory lesions, metabolism-based imaging often confuses malignant lesions with chronic inflammatory lesions.[20] Elevation of glucose metabolism is common in inflammatory lesions such as ulcerative colitis and Crohn's disease.[21] Even in the normal colon and rectum, there is a certain amount of physiological glucose uptake, which hampers the application of ^{18}F-FDG as a PET radiotracer in colorectal oncological imaging.[4] In addition, it is also difficult to distinguish the metastases of organs with high glucose metabolism, such as the brain.[6]

In this study, we provided a noninvasive oncological imaging modality for molecular imaging of CRC via targeting to integrin $\alpha6$. Early CRC with a localized stage can be successfully treated before distant metastasis occurs.[22] The ability to detect early colorectal lesions at a curable stage is the most important criterion for CRC screening. The overexpression of integrin $\alpha6$ in a majority of CRCs has been reported by several publications.[23−25] Elevation of this molecule occurs long before the changes in the anatomical structure when the tumor is visible to the naked eye. Most notably, integrin $\alpha6$, which plays an important role in proliferation of tumor cells, was found to be upregulated in more than 80% of CRCs in transcription levels.[24,25] The extremely high positive ratio of integrin $\alpha6$ in CRC makes it a good molecular imaging target for the sensitive detection of CRC. Moreover, Beaulieu et al.[26] found that the integrin $\alpha6$ subunit transcript (*ITGA6*) levels were significantly increased at all stages of CRC and could serve as a part of a stool assay to detect early colorectal lesions. The overexpression of integrin $\alpha6$ in the early stage of CRC enlightened us that PET imaging with ^{18}F-RWY may serve as a new approach for the detection of early CRC. On the other hand, PET/CT can determine whether there is early metastasis, thereby eliminating unnecessary examination in clinical practice.

Nevertheless, there are still several limitations of our study. First, as we can see in the results, the uptakes of the PET radiotracer ^{18}F-RWY in tumor and other tissues reach a peak in only a few minutes, and the rapid clearance of ^{18}F-RWY in vivo may reduce the sensitivity of CRC detection. The addition of modified chemical groups to alter its metabolism may prolong its half-life in vivo. Second, the binding affinity between RWY and integrin $\alpha6$ still need improvement. The affinity analysis between the synthesized integrin $\alpha6$ protein and RWY by surface plasmon resonance (SPR) is a direct method. One of our on-going studies is to improve the binding affinity via optimizing the peptide structure. Third, endoscopy is still the most commonly used method for the diagnosis of CRC currently. The gold standard for the diagnosis of CRC still depends on the pathological examination of tissue collected by endoscopy. Moreover, the high price of PET/CT imaging hampers its application as an early screening approach in clinical practice. However, from another point of view, this imaging will be beneficial for patients who need PET/CT examination during the perioperative period because the performance of PET/CT with our new radiopharmaceuticals can directly be used to diagnose and evaluate metastasis without the requirement of endoscopic examination anymore. Only a limited number of mice has been used for the detection of CRC. A series of clinical trials are needed to assess the effectiveness of this method in humans before it can be used clinically.

CONCLUSIONS

Integrin $\alpha6$ was overexpressed on several CRC cells and tumor tissues isolated from chemically induced and genetically engineered CRC mice. Integrin $\alpha6$ was the primary cellular target of RWY peptide, and the RWY peptide binds to CRC cells in vitro and in vivo. The integrin $\alpha6$-targeted peptide-based radiotracer ^{18}F-RWY is feasible for PET imaging of CRC in subcutaneous, chemically induced, and genetically engineered CRC mouse models, suggesting its future clinical applications.

EXPERIMENTAL SECTION

Cells and Animal Models. All the cell lines used in the experiment were obtained from the American Type Culture Collection (ATCC). Normal intestinal epithelial cell line FHC was cultured in Dulbecco's modified Eagle's medium: F-12 medium (ATCC 30-2006), and human colorectal adenocarcinoma cell line (HT29, LS-174T, RKO, HCT116, and SW620) was cultured in RPMI-1640 medium supplemented with 10% (v/v) fetal bovine serum, 100 U/mL penicillin, and 100 μg/mL streptomycin. The cells were maintained in an incubator with a humid atmosphere of 5% CO_2 at 37 °C. All mice were purchased from Vital River, Charles River Laboratories China (Beijing, China). The animal experiments were reviewed and approved by the animal welfare and ethics committees of Sun Yat-sen University Cancer Center. Approximately, 1×10^7 cells in a suspension with 20% Matrigel (Corning 354234, USA) were subcutaneously injected into the lateral thigh of BALB/c nude mice to create a subcutaneous tumor. To obtain a chemical-induced CRC mouse model, azoxymethane and dextran sulfate sodium were purchased from Sigma (St. Louis, MO) and administrated to C57BL6 mice based on the previous literature.[27] Mice were scanned by PET 80 days after drugs' induction. $Apc^{min/+}$ mice were purchased from The Jackson Laboratory (Bar Harbor, ME) and maintained under specific pathogen-free conditions in the Guangdong Pharmaceutical University Animal Experimental Center. Genotyping was tested by PCR with toe DNA using primers as follows: P1, 5′-TTCTGAGAAAGACAGAAGTTA-3′, together with P2, 5′-TTCCACTTTGGCATAAGGC-3′, was used to detect the mutant *Apc* allele (313 bp), which is only present in heterozygous $Apc^{min/+}$ mice. P3, 5′-GCCATCCCTTCACGTTAG-3′, together with the *Apc*-common primer, was used to detect the wild-type allele (619 bp).[28]

Biodistribution. To investigate the biodistribution of ^{18}F-RWY in vivo, the mice bearing HT29 were euthanized 60 min after intravenous injection of ^{18}F-RWY. Tumor and normal organs were collected, and the radioactivity was measured by a γ counter (Wallac Wizard 1470, PerkinElmer Inc.). The organs were weighed to calculate their mean organ distribution. Radioactivity was expressed as a percentage of the injected dose per gram [% ID/g, mean ± standard deviation (SD), n = 3/group].

DOI: 10.1021/acsomega.9b01920
ACS Omega 2019, 4, 15560−15566

PET/CT Imaging. The peptide powder previously freeze-dried was dissolved in saline and added to with 5 μL of acetic acid, 324 μL of ethanol and 370 MBq of fluoride ion (approximately 10 mCi). The mixture was boiled for 10 min and cooled to room temperature. The ^{18}F-RWY was captured by a C18 plus column (Waters, Sep-Pak, USA) because the free fluoride ion can pass through the column. After being washed with saline twice, the peptide was eluted with 400 μL of ethanol, and the obtained solution was blown in nitrogen until the liquid was almost evaporated. A volume of 200 μL saline was added after the radioactivity was measured. Mice were anesthetized with 2.5% tribromoethanol (T48402, Sigma-Aldrich, Germany) and intravenously injected with approximately 3.7 MBq (100 μCi) of ^{18}F-RWY or ^{18}F-FDG. PET/CT was performed after 1 h in vivo circulation with the imaging agent. To analyze the enrichment of the tracer in the tumor, regions of interest were drawn on tumors in three dimensions, and the maximum uptake value was calculated. The tumor and tissue densities were assumed as 1 g/cm^3, and its uptake is presented as the % ID/g and was calculated by measuring the tumor and tissue radioactivity. To perform dynamic imaging, the images were acquired as follows: 1 × 5, 1 × 25, 9 × 30, 5 × 60, 5 × 120, and 9 × 240 s. Time activity curves were obtained according to the pharmacokinetics of ^{18}F-RWY in the tumors and other organs. The uptake of the tracer was quantified as SUV.

Immunohistochemistry. Tumors from mouse models were carefully dissected, fixed with formalin, and embedded with paraffin. Paraffin blocks were cut into 3 mm sections and some were stained with hematoxylin and eosin (H&E). The remaining sections were deparaffinized in xylene and dehydrated by serial immersion in 100, 90, 80, and 70% ethanol and distilled water. Antigen retrieval was performed under high pressure with boiling citrate buffer (10 mM, pH 9.0) for 3 min. All samples were blocked with 5% bovine serum albumin and incubated with anti-integrin α6 antibody (Abcam, ab181551) at a dilution of 1:150 overnight at 4 °C. After washing with PBST three times, the samples were incubated with an HRP-conjugated rabbit anti-mouse monoclonal secondary antibody at a dilution of 1:200 at 25 °C for 30 min. Finally, the chromogenic reaction was performed using the DAB Kit (Zhongshan Jinqiao, ZLI-9017, China). Images were visualized and captured by a microscope (Nikon Eclipse, Japan) at 10× and 20× magnification.

Immunofluorescence. Approximately 1 × 10^5 HT29 cells were plated on coverslips and added to 80 μM biotin-labeled peptide. After a 4 h incubation at 37 °C, the coverslips were washed with PBST five times, fixed with 4% paraformaldehyde, incubated with PBS containing 0.25% Triton X-100 (Sigma-Aldrich, Germany), and blocked with 5% BSA for half an hour. Antibody incubation was performed with anti-integrin α6 antibody (Abcam, ab181551) at a dilution of 1:1000 overnight at 4 °C. To detect the fluorescence, the samples were incubated with both streptavidin-Cy3 (Thermo Fisher 434315, USA) and goat anti-mouse Alexa Fluor 488 secondary antibody (Abcam, ab150113) at a dilution of 1:1000 in 1% BSA for 1 h at room temperature in the dark. The samples were incubated with 1 μg/mL DAPI, and the coverslips were mounted with ProLong Gold antifade (Invitrogen P26930, USA). Fluorescence images were visualized and captured by a confocal microscopy confocal laser-scanning system (Olympus FV1000, Japan) at 40× and 100× magnification. Colocalization was analyzed with ImageJ (http://rsbweb.nih.gov/ij/) and the colocalization finder plug-in.

Data Analysis and Statistics. Statistical analyses were performed using Prism 7.0 (GraphPad, San Diego, USA). All data were presented as the mean ± SD. The *P*-values were tested for significance using the two-sided Student *t*-test. *P*-values less than 0.05 were considered to be statistically significant ($^*p < 0.05$, $^{**}p < 0.01$).

■ ASSOCIATED CONTENT

Supporting Information

The Supporting Information is available free of charge on the ACS Publications website at DOI: 10.1021/acsomega.9b01920.

Stability in vitro of ^{18}F-RWY analyzed by HPLC, 3D model PET/CT image with ^{18}F-RWY in a chemically induced CRC mouse, 3D model PET/CT image with ^{18}F-RWY in a genetically engineered CRC mouse, and PET/CT imaging with ^{18}F-FDG in a genetically engineered CRC mouse (PDF)

■ AUTHOR INFORMATION

Corresponding Authors

*E-mail: lijj@sysucc.org.cn. Phone: +8620 8734 3106 (J.-J.L.).
*E-mail: fengguok@sysucc.org.cn. Phone: +8620 8734 3169 (G.-K.F.).

ORCID

Guo-Kai Feng: 0000-0002-8251-291X

Author Contributions

‖Y.-T.X., C.Z., and J.-C.Y. contributed equally to this work.

Notes

The authors declare no competing financial interest.
The authenticity of this article has been validated by uploading the key raw data onto the Research Data Deposit public platform (www.researchdata.org.cn), with the approval RDD number as RDDB2019000585.

■ ACKNOWLEDGMENTS

This work was supported by grants from the National Key R&D Program of China (2017YFA0505600 and 2016YFA0502100), the National Natural Science Foundation of China (NSFC) (projects 81602364, 81621004, 81520108022, 81572403) and the Science and Technology Project of Guangdong Province (2014B020210002 and 2017A020211010), the Health and Medical Collaborative Innovation Project of Guangzhou City, China (201400000001 and 20150802024), and the Sci-Tech Project Foundation of Guangzhou City (201607020038 and 201803040015).

■ REFERENCES

(1) Bray, F.; Ferlay, J.; Soerjomataram, I.; Siegel, R. L.; Torre, L. A.; Jemal, A. Global Cancer Statistics 2018: GLOBOCAN Estimates of Incidence and Mortality Worldwide for 36 Cancers in 185 Countries. *Ca-Cancer J. Clin.* **2018**, *68*, 394−424.
(2) Brenner, H.; Kloor, M.; Pox, C. P. Colorectal Cancer. *Lancet* **2014**, *383*, 1490−1502.
(3) Higashikawa, K.; Akada, N.; Yagi, K.; Watanabe, K.; Kamino, S.; Kanayama, Y.; Hiromura, M.; Enomoto, S. Exploration of Target Molecules for Molecular Imaging of Inflammatory Bowel Disease. *Biochem. Biophys. Res. Commun.* **2011**, *410*, 416−421.
(4) Heriot, A. G.; Hicks, R. J.; Drummond, E. G. P.; Keck, J.; Mackay, J.; Chen, F.; Kalff, V. Does Positron Emission Tomography

DOI: 10.1021/acsomega.9b01920
ACS Omega 2019, 4, 15560−15566

Change Management in Primary Rectal Cancer? A Prospective Assessment. *Dis. Colon Rectum* **2004**, *47*, 451−458.
(5) Turker, N. S.; Heidari, P.; Kucherlapati, R.; Kucherlapati, M.; Mahmood, U. An EGFR Targeted PET Imaging Probe for the Detection of Colonic Adenocarcinomas in the Setting of Colitis. *Theranostics* **2014**, *4*, 893−903.
(6) Purandare, N. C.; Puranik, A.; Shah, S.; Agrawal, A.; Gupta, T.; Moiyadi, A.; Shetty, P.; Shridhar, E.; Jalali, R.; Rangarajan, V. Common malignant brain tumors. *Nucl. Med. Commun.* **2017**, *38*, 1109−1116.
(7) Desgrosellier, J. S.; Cheresh, D. A. Integrins in Cancer: Biological Implications and Therapeutic Opportunities. *Nat. Rev. Cancer* **2010**, *10*, 9−22.
(8) Begum, N. A.; Mori, M.; Matsumata, T.; Takenaka, K.; Sugimachi, K.; Barnard, G. F. Differential Display and Integrin Alpha 6 Messenger RNA Overexpression in Hepatocellular Carcinoma. *Hepatology* **1995**, *22*, 1447−1455.
(9) Wang, Y.; Shenouda, S.; Baranwal, S.; Rathinam, R.; Jain, P.; Bao, L.; Hazari, S.; Dash, S.; Alahari, S. K. Integrin Subunits Alpha5 and Alpha6 Regulate Cell Cycle by Modulating the Chk1 and Rb/E2F Pathways to Affect Breast Cancer Metastasis. *Mol. Cancer* **2011**, *10*, 84.
(10) Grossman, H. B.; Lee, C.; Bromberg, J.; Liebert, M. Expression of the Alpha6beta4 Integrin Provides Prognostic Information in Bladder Cancer. *Oncol. Rep.* **2000**, *7*, 13−19.
(11) Feng, G.-K.; Zhang, M. Q.; Wang, H. X.; Cai, J.; Chen, S. P.; Wang, Q.; Gong, J.; Leong, K. W.; Wang, J.; Zhang, X.; Zeng, M. S. Identification of an Integrin α6-Targeted Peptide for Nasopharyngeal Carcinoma-Specific Nanotherapeutics. *Adv. Ther.* **2019**, *2*, 1900018.
(12) Ramos, D. M.; Dang, D.; Sadler, S. The Role of the Integrin Alpha v Beta6 in Regulating the Epithelial to Mesenchymal Transition in Oral Cancer. *Anticancer Res.* **2009**, *29*, 125−130.
(13) Agrez, M.; Chen, A.; Cone, R. I.; Pytela, R.; Sheppard, D. The Alpha v Beta 6 Integrin Promotes Proliferation of Colon Carcinoma Cells through a Unique Region of the Beta 6 Cytoplasmic Domain. *J. Cell Biol.* **1994**, *127*, 547−556.
(14) Liu, Z.; Niu, G.; Wang, F.; Chen, X. 68Ga-labeled NOTA-RGD-BBN peptide for dual integrin and GRPR-targeted tumor imaging. *Eur. J. Nucl. Med. Mol. Imaging* **2009**, *36*, 1483−1494.
(15) Dmochowska, N.; Wardill, H. R.; Hughes, P. A. Advances in Imaging Specific Mediators of Inflammatory Bowel Disease. *Int. J. Mol. Sci.* **2018**, *19*, 2471.
(16) Misawa, M.; Kudo, S.-E.; Mori, Y.; Cho, T.; Kataoka, S.; Yamauchi, A.; Ogawa, Y.; Maeda, Y.; Takeda, K.; Ichimasa, K.; Nakamura, H.; Yagawa, Y.; Toyoshima, N.; Ogata, N.; Kudo, T.; Hisayuki, T.; Hayashi, T.; Wakamura, K.; Baba, T.; Ishida, F.; Itoh, H.; Roth, H.; Oda, M.; Mori, K. Artificial Intelligence-Assisted Polyp Detection for Colonoscopy: Initial Experience. *Gastroenterology* **2018**, *154*, 2027−2029.e3.
(17) van Rijn, J. C.; Reitsma, J. B.; Stoker, J.; Bossuyt, P. M.; van Deventer, S. J.; Dekker, E. Polyp Miss Rate Determined by Tandem Colonoscopy: A Systematic Review. *Am. J. Gastroenterol.* **2006**, *101*, 343−350.
(18) Lee, S. Y.; Jeon, S. I.; Jung, S.; Chung, I. J.; Ahn, C.-H. Targeted Multimodal Imaging Modalities. *Adv. Drug Delivery Rev.* **2014**, *76*, 60−78.
(19) Wang, Q.; Li, S.-B.; Zhao, Y.-Y.; Dai, D.-N.; Du, H.; Lin, Y.-Z.; Ye, J.-C.; Zhao, J.; Xiao, W.; Mei, Y.; Xiao, Y.-T.; Liu, S.-C.; Li, Y.; Xia, Y.-F.; Song, E.-W.; Tang, G.-H.; Zhang, W.-G.; Li, Z.-J.; Zheng, X.-B.; Cao, D.-H.; Li, M.-Z.; Zhong, Q.; Chen, Z.-P.; Qian, C.-N.; Fan, W.; Feng, G.-K.; Zeng, M.-S. Identification of a sodium pump Na + /K + ATPase α1-targeted peptide for PET imaging of breast cancer. *J. Controlled Release* **2018**, *281*, 178−188.
(20) Strauss, L. G. Fluorine-18 Deoxyglucose and False-Positive Results: A Major Problem in the Diagnostics of Oncological Patients. *Eur. J. Nucl. Med.* **1996**, *23*, 1409−1415.
(21) Halpenny, D. F.; Burke, J. P.; Lawlor, G. O.; O'Connell, M. Role of PET and Combination PET/CT in the Evaluation of Patients with Inflammatory Bowel Disease. *Inflammatory Bowel Dis.* **2009**, *15*, 951−958.
(22) Maratt, J. K.; Saini, S. D. Colorectal cancer screening in the 21st century: where do we go from here? *Am J Manag Care* **2015**, *21*, e447−9.
(23) Ni, H.; Dydensborg, A. B.; Herring, F. E.; Basora, N.; Gagné, D.; Vachon, P. H.; Beaulieu, J.-F. Upregulation of a functional form of the β4 integrin subunit in colorectal cancers correlates with c-Myc expression. *Oncogene* **2005**, *24*, 6820−6829.
(24) Dydensborg, A. B.; Teller, I. C.; Groulx, J.-F.; Basora, N.; Pare, F.; Herring, E.; Gauthier, R.; Jean, D.; Beaulieu, J.-F. Integrin Alpha6Bbeta4 Inhibits Colon Cancer Cell Proliferation and C-Myc Activity. *BMC Cancer* **2009**, *9*, 223.
(25) Groulx, J.-F.; Giroux, V.; Beauséjour, M.; Boudjadi, S.; Basora, N.; Carrier, J. C.; Beaulieu, J.-F. Integrin α6A splice variant regulates proliferation and the Wnt/β-catenin pathway in human colorectal cancer cells. *Carcinogenesis* **2014**, *35*, 1217−1227.
(26) Beaulieu, J.-F.; Herring, E.; Kanaoka, S.; Tremblay, É. Use of Integrin Alpha 6 Transcripts in a Stool MRNA Assay for the Detection of Colorectal Cancers at Curable Stages. *Oncotarget* **2016**, *7*, 14684−14692.
(27) Neufert, C.; Becker, C.; Neurath, M. F. An inducible mouse model of colon carcinogenesis for the analysis of sporadic and inflammation-driven tumor progression. *Nat. Protoc.* **2007**, *2*, 1998−2004.
(28) Ju, J.; Hong, J.; Zhou, J.-n.; Pan, Z.; Bose, M.; Liao, J.; Yang, G.-y.; Liu, Y. Y.; Hou, Z.; Lin, Y.; Ma, J.; Shih, W. J.; Carothers, A. M.; Yang, C. S. Inhibition of Intestinal Tumorigenesis inApcmin/+Mice by (−)-Epigallocatechin-3-Gallate, the Major Catechin in Green Tea. *Cancer Res.* **2005**, *65*, 10623−10631.

DOI: 10.1021/acsomega.9b01920
ACS Omega 2019, 4, 15560−15566